Irradiation-induced disordering and amorphization of Al_3Ti-based intermetallic compounds

Jeong-Yong Park [a, *], Il-Hyun Kim [a], Arthur T. Motta [b], Christopher J. Ulmer [b], Marquis A. Kirk Jr. [c], Edward A. Ryan [c], Peter M. Baldo [c]

[a] LWR Fuel Technology Division, Korea Atomic Energy Research Institute, 989-111 Daedeok-daero, Yuseong-gu, Daejeon 305-353, Republic of Korea
[b] Department of Mechanical and Nuclear Engineering, The Pennsylvania State University, 227 Reber Building, University Park, PA 16802, USA
[c] Electron Microscopy Center, Nuclear Engineering Division, Argonne National Laboratory, Argonne, IL 60439, USA

ARTICLE INFO

ABSTRACT

An in situ ion-irradiation study, simultaneously examined using transmission electron microscopy, was performed to investigate irradiation-induced disordering and amorphization of Al_3Ti-based intermetallic compounds. Thin foil samples of two crystalline structures: $D0_{22}$-structured Al_3Ti and $L1_2$-structured $(Al,Cr)_3Ti$ were irradiated using 1.0 MeV Kr ions at a temperature range from 40 K to 573 K to doses up to 4.06×10^{15} ions/cm^2. The results showed that both the compounds underwent an order-disorder transformation under irradiation, where both Al_3Ti and $(Al,Cr)_3Ti$ ordered structures were fully transformed to the disordered face-centered cubic (FCC) structure except at the highest irradiation temperature of 573 K. A slightly higher irradiation dose was required for order-disorder transformation in case of Al_3Ti as compared to $(Al,Cr)_3Ti$ at a given temperature. However, their amorphization resistances were different: while the disordered FCC $(Al,Cr)_3Ti$ amorphized at the irradiation dose of 6.25×10^{14} ions/cm^2 (0.92 dpa) at 40 K and 100 K, the Al_3Ti compound with the same disordered FCC structure maintained crystallinity up to 4.06×10^{15} ions/cm^2 (5.62 dpa) at 40 K. The critical temperature for amorphization of $(Al,Cr)_3Ti$ under Kr ion irradiation is likely between 100 K and room temperature and the critical temperature for disordering between room temperature and 573 K.

© 2015 Elsevier B.V. All rights reserved.

1. Introduction

Al_3Ti intermetallic compounds have been proposed as a potential high-temperature structure material because of their low density (3.36 g/cm^3), relatively high melting temperature (>1623 K), and good oxidation resistance [1]. The main obstacle to employing Al_3Ti as a structural material is its brittleness that is intrinsically caused by a non-symmetrical (tetragonal) $D0_{22}$ crystal structure having insufficient independent slip systems for plastic deformation [2]. The $D0_{22}$-structured Al_3Ti can be transformed to the more symmetric $L1_2$ structure by replacing some of the Al with transition metals [3–6]. The $L1_2$ structure features improved ductility because the increased number of independent slip systems in the cubic structure improves tensile ductility when deformed at low temperatures [7].

Fig. 1 shows the unit cells of $D0_{22}$ and $L1_2$ ordered structures. The tetragonal $D0_{22}$ structure is derived from the cubic $L1_2$ structure by introducing an anti-phase boundary on every (001) plane. Under equilibrium conditions, Al_3Ti is stabilized into the relatively non-symmetrical $D0_{22}$ structure (instead of the more symmetrical $L1_2$ structure) primarily due to the fact that the hybridization between Al p and Ti d electrons results in a strong directionality of bonding structure. The stability of $D0_{22}$ relative to $L1_2$ varies depending on the c/a ratio, according to ab initio calculations performed using the augmented-spherical-wave (ASW) method [8]. The energy of the binary Al_3Ti compound with $D0_{22}$ structure was found to be lower than that with $L1_2$ structure by about 0.05 eV/atom (4800 J/g-atom) when the c/a ratio was increased (relaxed) to 2.24, while, for the ideal c/a ratio of 2, $L1_2$ was more stable than $D0_{22}$.

One possible application of Al_3Ti-based intermetallic compounds is in the fabrication of oxidation-resistant coatings for nuclear fuel cladding to enhance accident tolerance [9] as they show excellent oxidation resistance in high-temperature environments

* Corresponding author.
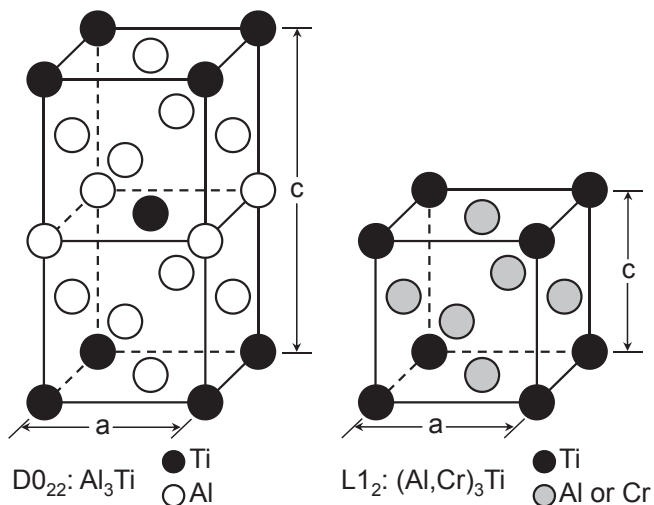E-mail address: parkjy@kaeri.re.kr (J.-Y. Park).

Fig. 1. Unit cells of $D0_{22}$ and $L1_2$ ordered structures.

[10,11]. Prior to application in nuclear reactors, it is crucial to clarify the effect of irradiation on the properties of Al_3Ti-based intermetallic compounds. However, no work has been carried out on the effect of irradiation on phase stability of Al_3Ti-based alloys except that the $D0_{22}$-structured Al_3Ti was reported to undergo amorphization at 1.3 dpa under 250 keV Kr ion irradiation at temperatures less than 40 K [12]. Moreover, $L1_2$-structured Al_3Ti-based ternary alloys, which are more suitable for coating applications in the light of their higher ductility, are anticipated to show a different behavior under irradiation than $D0_{22}$-structured binary Al_3Ti.

In general, intermetallic compounds have been reported to undergo disordering and amorphization under irradiation [13,14] due to chemical and topological disordering [14]. The use of Al_3Ti-based intermetallic compounds in fuel claddings requires a more fundamental understanding of the phase stability in the irradiation condition. It is crucial to clarify how Al_3Ti-based intermetallic compounds behave in terms of disordering, phase change, and susceptibility to amorphization under irradiation. The objective of this work is to investigate phase stability and susceptibility to amorphization under irradiation at various temperatures for Al_3Ti-based intermetallic compounds, with focus on the different response in terms of amorphization and disordering of the two crystal structures: $D0_{22}$ and $L1_2$.

2. Experimental procedure

Two types of Al_3Ti-based intermetallic compounds with different crystal structures were used in this study: Al_3Ti with $D0_{22}$ and $(Al,Cr)_3Ti$ with $L1_2$. Ingots were manufactured by arc melting of mixtures with compositions of Al−25Ti and Al−25Ti−10Cr (at.%) followed by homogenizing at 1423 K for 48 h to obtain the desired crystal structures of $D0_{22}$ for Al_3Ti and $L1_2$ for $(Al,Cr)_3Ti$, respectively. Samples for in situ transmission electron microscopy (TEM) under ion irradiation were prepared by the following procedure: the homogenized ingots were cut into sheet-type specimens, mechanically polished down to a thickness of about 100 μm, punched out into 3 mm discs, and perforated by electro-polishing on both sides in a solution of 10% perchloric acid and 90% methanol at 253 K and 20 V.

The electron-transparent samples were irradiated with 1.0 MeV Kr ions at a dose rate of 6.25×10^{11} ions/cm^2-s using the IVEM-Tandem, a facility in the Electron Microscopy Center in the

Argonne National Laboratory, in which a Hitachi 9000 transmission electron microscope is linked to an ion implanter. Ion irradiations were carried out at temperatures of 40 K, 100 K, 298 K (room temperature), and 573 K to examine the effect of temperature on the phase transformations of the crystal structure. The displacement damage distribution as a function of depth was calculated using the Monte Carlo software package SRIM [15]. Fig. 2 shows the SRIM calculation results for Al_3Ti and $(Al,Cr)_3Ti$ using the Kinchin-Pease model [16] with a mean threshold displacement energy $E_d = 28$ eV [12] for Al, Ti, and Cr. During the irradiation at each temperature, the changes in the material microstructures and diffraction patterns were observed in situ. Irradiations were systematically stopped at certain dose levels to acquire bright-field and dark-field images, and diffraction patterns using the Gatan Digital Micrographs software.

3. Results and discussion

Fig. 3 shows selected area diffraction patterns of Al_3Ti before and after irradiation with 1.0 MeV Kr ions at a rate of 6.25×10^{11} ions/cm^2-s at 40 K and room temperature, which, according to SRIM calculation, produces a displacement rate of approximately 5×10^{-3}/s, proportionally divided between Al and Ti. Fig. 3a shows an Al_3Ti diffraction pattern taken before the irradiation which shows an ordered crystal structure of $D0_{22}$ at 40 K. Both superlattice reflections and fundamental reflections were visible before the irradiation. The ratio of the intensity of the superlattice reflections to that of the fundamental reflections decreased as the irradiation dose increased to 6.25×10^{13} ions/cm^2 (0.09 dpa) (Fig. 3b), indicating that the irradiation caused disordering of the initially ordered crystal structure. The order-disorder transformation was found to be completed at the irradiation of 3.13×10^{14} ions/cm^2 (0.43 dpa) (Fig. 3c), as at that dose the superlattice reflections disappeared and the remaining fundamental reflections were identified as face-centered cubic (FCC). The disordered FCC structure was irradiated to a dose of 4.06×10^{15} ions/cm^2 (5.62 dpa) with no change in the diffraction pattern and in particular, no amorphization being observed (Fig. 3d).

The results of the irradiation-induced phase transformation at room temperature were similar to those observed at 40 K, except that the irradiation dose for the completion of order-disorder
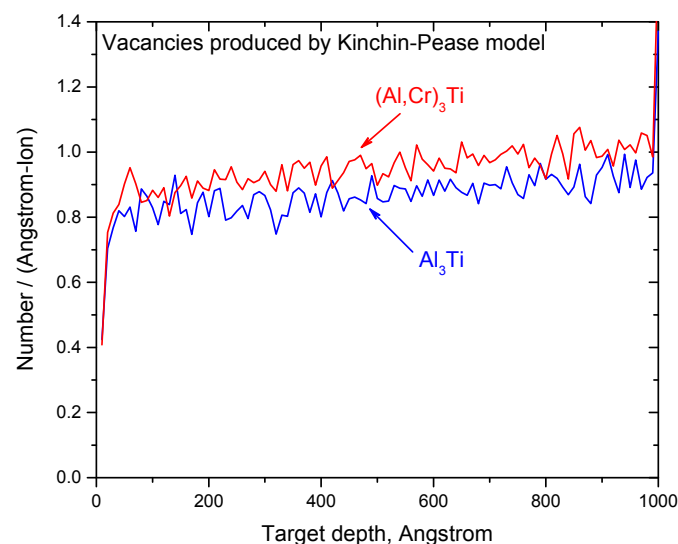

Fig. 2. SRIM calculation results for Al_3Ti and $(Al,Cr)_3Ti$ using the Kinchin-Pease model with a mean threshold displacement energy $E_d = 28$ eV for Al, Ti, and Cr.
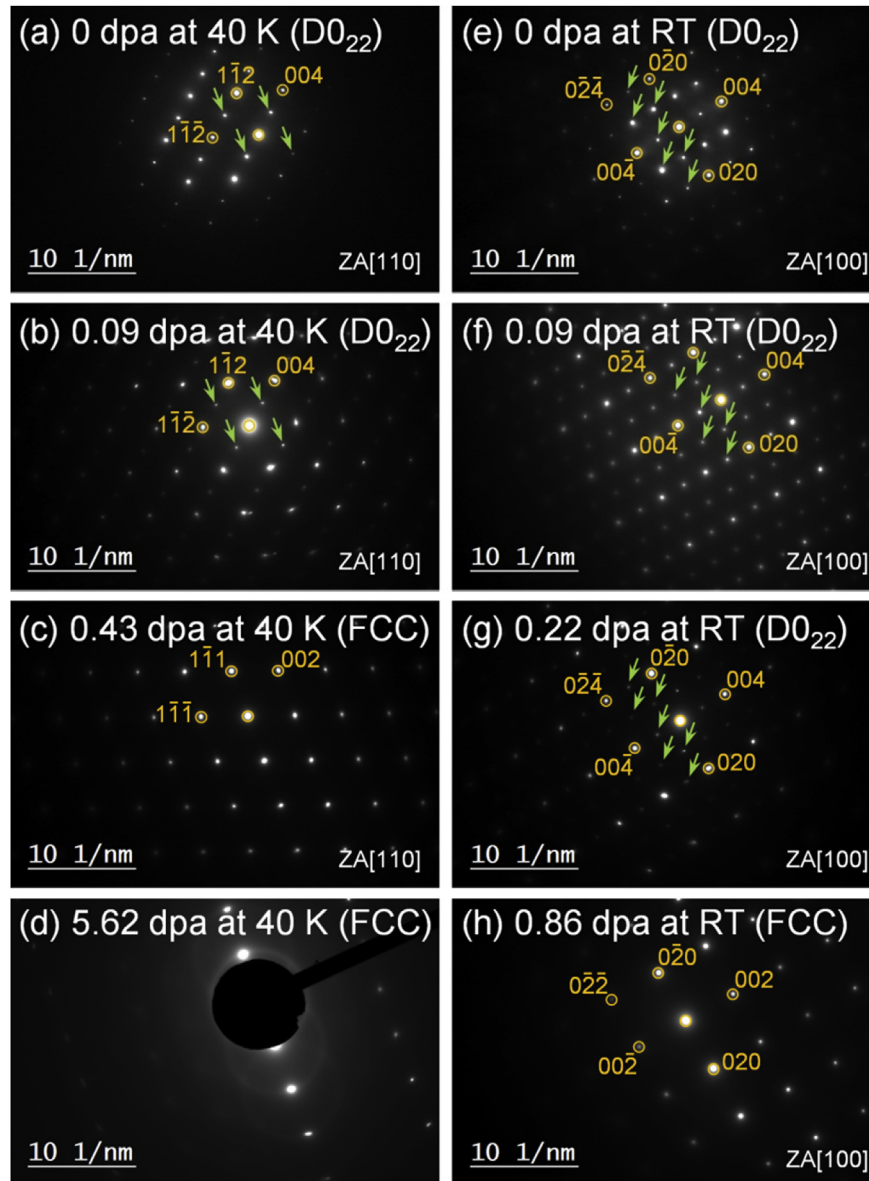
Fig. 3. Selected area diffraction patterns of Al_3Ti before and after irradiation with 1.0 MeV Kr ions at a rate of 6.25×10^{11} ions/cm²-s at 40 K and room temperature (RT). Open circles and arrows indicate fundamental and superlattice reflections, respectively.

transformation increased up to 6.25×10^{14} ions/cm² (0.86 dpa) (Fig. 3h). The ordered crystal structure of $D0_{22}$ became increasingly disordered with higher irradiation dose, which is confirmed by the fact that the intensity of the superlattice reflections became weaker as the irradiation dose increased from 0 up to 1.56×10^{14} ions/cm² (0.22 dpa), eventually changing to the disordered FCC structure. The irradiation at room temperature was ended at 6.25×10^{14} ions/cm² (0.86 dpa) when the ordered structure of $D0_{22}$ was fully transformed to the disordered FCC structure.

The irradiation-induced phase transformation was also investigated for the $(Al,Cr)_3Ti$ sample which has a $L1_2$ crystal structure. Fig. 4 shows the selected area diffraction patterns (a, c, d, f) and the transmission electron micrographs (b, e) of $(Al,Cr)_3Ti$ before and after irradiation with 1.0 MeV Kr ions at a rate of 6.25×10^{11} ions/cm²-s at 40 K. The diffraction pattern obtained before irradiation exhibited a fully ordered structure of $L1_2$ with both fundamental and superlattice reflections visible (Fig. 4a) and an absence of defects or imperfections (Fig. 4b). As the irradiation dose increased up

to 6.25×10^{13} ions/cm² (0.09 dpa), the intensity of superlattice reflections decreased (Fig. 4c), finally disappearing at a dose of 1.56×10^{14} ions/cm² (0.23 dpa). In Fig. 4d, an amorphous ring is also visible together with the diffraction pattern on FCC, indicating that the ordered $L1_2$ structure has fully transformed to the disordered FCC structure before this dose level. Many defects are visible in the irradiated microstructure up to a dose of 1.56×10^{14} ions/cm² (0.23 dpa) (Fig. 4e). The dose to the completion of order-disorder transformation was lower in $(Al,Cr)_3Ti$ compared to Al_3Ti at 40 K. The disordered FCC $(Al,Cr)_3Ti$ eventually amorphized as the irradiation dose increased up to 6.25×10^{14} ions/cm² (0.92 dpa) (Fig. 4f), whereas Al_3Ti remained crystalline up to 4.06×10^{15} ions/cm² (5.62 dpa).

Fig. 5 shows selected area diffraction patterns of $(Al,Cr)_3Ti$ before and after irradiation with 1.0 MeV Kr ions at a rate of 6.25×10^{11} ions/cm²-s at 100 K. As the irradiation dose increased, the initial ordered structure of $L1_2$ became disordered, fully transforming to the disordered FCC at 2.19×10^{14} ions/cm² (0.32 dpa)
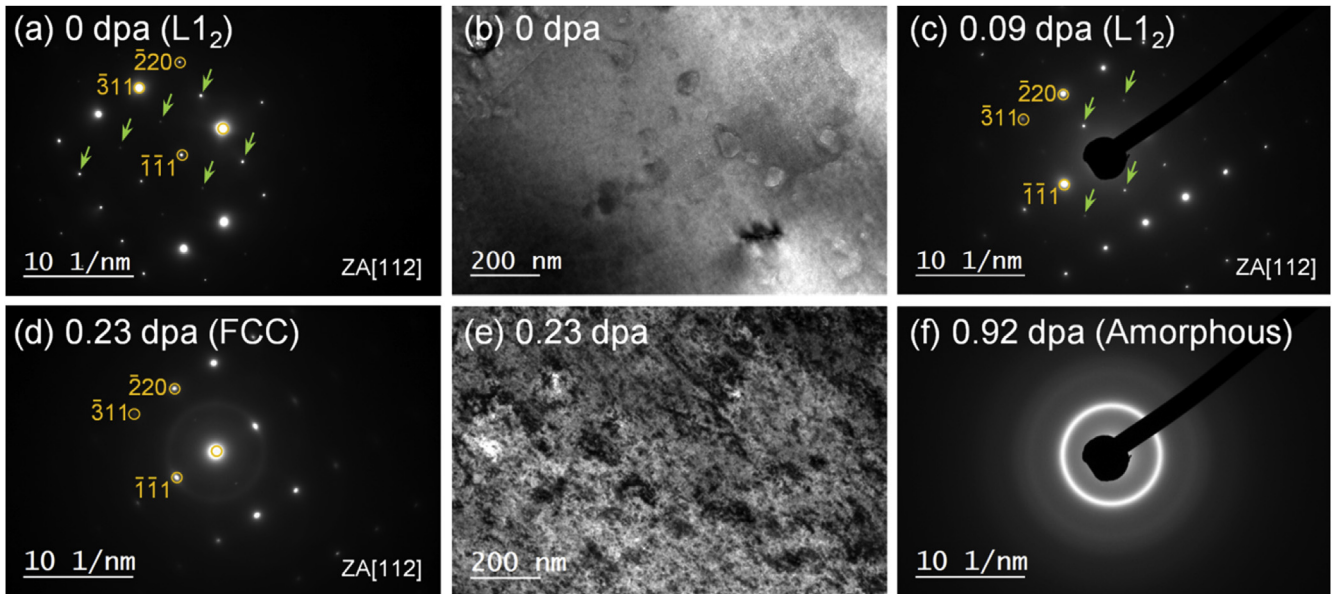
Fig. 4. Selected area diffraction patterns (a, c, d, f) and transmission electron micrographs (b, e) of (Al,Cr)$_3$Ti before and after irradiation with 1.0 MeV Kr ions at a rate of 6.25 $\times$ 10^{11} ions/cm^2-s at 40 K. Open circles and arrows indicate fundamental and superlattice reflections, respectively.

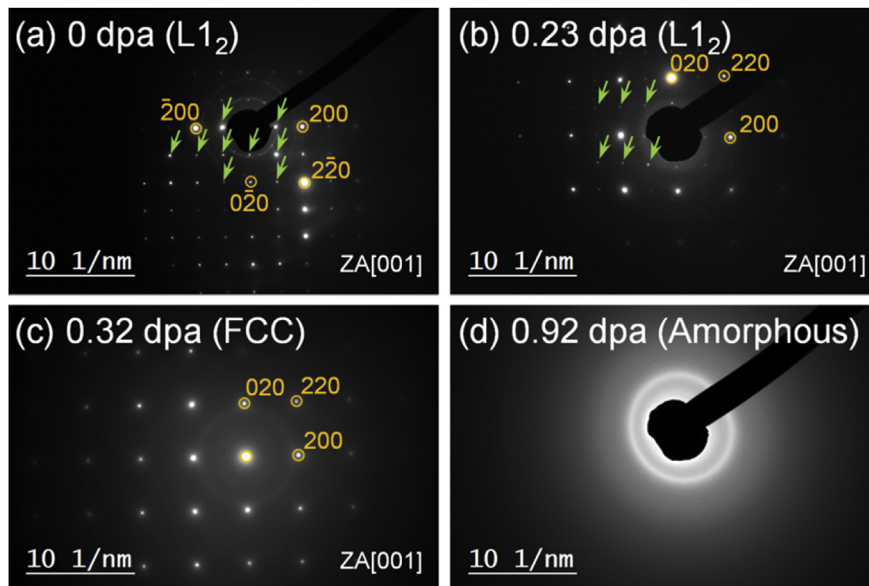**Fig. 5.** Selected area diffraction patterns of (Al,Cr)$_3$Ti before and after irradiation with 1.0 MeV Kr ions at a rate of 6.25 $\times$ 10^{11} ions/cm^2-s at 100 K. Open circles and arrows indicate fundamental and superlattice reflections, respectively.

and finally amorphizing at 6.25 $\times$ 10^{14} ions/cm^2 (0.92 dpa). The trend of the phase transformation observed in Fig. 5 was, in general, similar to the behavior shown in Fig. 4 except that the irradiation dose for the completion of the order-disorder transformation increased from 1.56 $\times$ 10^{14} ions/cm^2 (0.23 dpa) to 2.19 $\times$ 10^{14} ions/cm^2 (0.32 dpa) with the increase of the irradiation temperature from 40 K to 100 K. The critical dose to amorphization could not be precisely detected at 40 K and 100 K although it is clear that amorphization was complete at an irradiation dose of 6.25 $\times$ 10^{14} ions/cm^2 (0.92 dpa) at both temperatures.

When the irradiation temperature was increased to room temperature, the irradiation dose to the order-disorder transformation of (Al,Cr)$_3$Ti increased up to 2.50 $\times$ 10^{14} ions/cm^2 (0.37 dpa)

(Fig. 6b). It can be noted that the L1$_2$-structured (Al,Cr)$_3$Ti was not amorphized by the Kr ion irradiation up to 3.13 $\times$ 10^{15} ions/cm^2 (4.60 dpa) at room temperature. In the irradiation experiment at 573 K, although some irradiation-induced disordering of (Al,Cr)$_3$Ti was observed when the material was subjected to a dose of 3.13 $\times$ 10^{15} ions/cm^2 (4.60 dpa), the transformation was not complete. The superlattice reflections were still prominent in the diffraction pattern shown in Fig. 6f, even though the relative intensity of superlattice reflections to the fundamental ones became weaker compared to that for the unirradiated specimen.

Fig. 7 shows a summary of the results of the experiments conducted in a plot of irradiation dose (ions/cm^2) versus irradiation temperature for Al$_3$Ti and (Al,Cr)$_3$Ti. Both compounds become
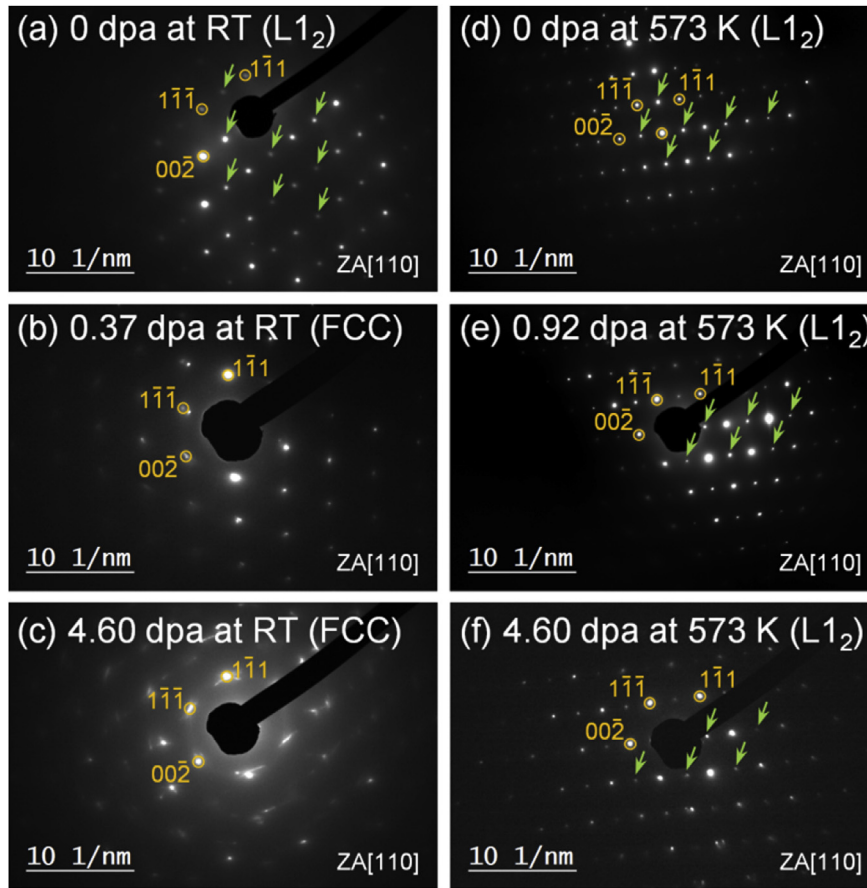
Fig. 6. Selected area diffraction patterns of $(Al,Cr)_3Ti$ before and after irradiation with 1.0 MeV Kr ion at a rate of 6.25×10^{11} ions/cm^2-s at room temperature (RT) and 573 K. Open circles and arrows indicate fundamental and superlattice reflections, respectively.
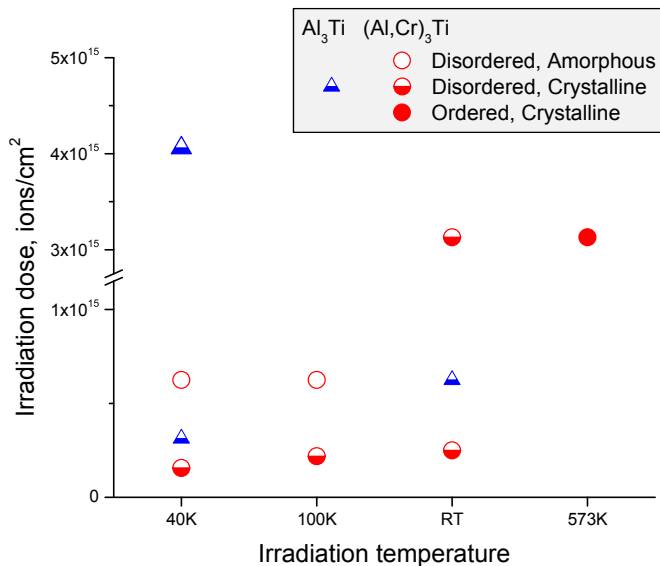

Fig. 7. Irradiation dose to order–disorder transformation and amorphization as a function of irradiation temperature for Al_3Ti and $(Al,Cr)_3Ti$.

chemically disordered at all temperatures but the highest temperature (573 K). At low temperatures (40 and 100 K), $(Al,Cr)_3Ti$ becomes amorphous after irradiation to roughly twice the dose needed for chemical disordering, while Al_3Ti resisted

amorphization even to a dose ten times as much that for chemical disordering. This indicates that chemical disordering is not sufficient to cause amorphization in these compounds, and further accumulation of damage might be required. It also appears that the damage accumulation processes at low temperatures are more efficient for $(Al,Cr)_3Ti$ than for Al_3Ti. Finally, the critical temperature for amorphization for $(Al,Cr)_3Ti$ is likely to be between 100 K and room temperature while the critical temperature for disordering for $(Al,Cr)_3Ti$ is likely between room temperature and 573 K.

In a previous study [12], D0$_{22}$-structured Al_3Ti was reported to be completely amorphized at around 1.3 dpa by 250 keV Kr ion irradiation at temperatures less than 40 K. In this study, however, Al_3Ti was not amorphized when irradiated with 1.0 MeV Kr ions to a higher dose level, 5.62 dpa, at 40 K. The irradiation condition was similar in both experiments apart from a higher ion energy in the current study. The different resistance to amorphization found in the two experiments is difficult to understand in terms of the irradiation conditions only. The susceptibility to amorphization could be influenced by the materials' chemical homogeneity, which might be altered in the two experiments due to the different manufacturing conditions.

The binary phase diagram for Ti–Al system indicates that Al_3Ti is a line compound, suggesting that Al_3Ti is not stable under irradiation conditions. Nakayama et al. reported that the L1$_2$ phase field in the isothermal section at 1273 K of the A1-Ti-Cr ternary phase diagram is very narrow with about 1 at% radius and its center at Al−25Ti−8Cr, and the extent of the L1$_2$ phase field increased toward higher content of Cr and Ti at 1423 K [3]. This suggests that

the L1$_2$ phase is not stable at the irradiation temperatures used in this study even though the L1$_2$ phase was obtained in this study by annealing at 1423 K for 48 h. From this point of view, L1$_2$-(Al,Cr)$_3$Ti is more likely to transform to another phase under irradiation compared to D0$_{22}$-Al$_3$Ti, which maintains a stable line compound in the temperature range used in this study before irradiation.

The free energy increase by irradiation should be higher than the difference between the initial ordered phase and disordered or amorphous phase in order for the transformation to take place. A certain amount of energy needs to be stored in the lattice during the irradiation, though most energy can be dissipated as heat. Two most commonly accepted forms for accumulation of energy are chemical disordering (anti-site defect) and topological disordering (point defect). Chemical disordering is accepted as the major energy storage form [17], but point defects also contributes to the energy storage [18,19]. Tolerance to radiation damage is a material's inherent ability to accommodate atomic lattice disorder under irradiation [20] and its damage annealing rate. This ability is closely associated with the increase of free energy by irradiation-induced defects. When the energy change by defect formation is large, the materials can undergo an order-disorder transformation or amorphization.

The current study showed that Al$_3$Ti is much more resistant to amorphization under irradiation compared with (Al,Cr)$_3$Ti. The resistance to amorphization is enhanced if the stored energy due to the accumulation of irradiation-induced defects is reduced. Intrinsically disordered materials tend to remain disordered throughout the irradiation process. A low energy for the order-disorder transformation helps the materials accommodate disorder more easily [20]. L1$_2$-(Al,Cr)$_3$Ti is a more disordered structure compared to D0$_{22}$, considering that Al and Cr atoms can share face-centered lattice positions in the L1$_2$ unit cell as shown in Fig. 1. The current study, however, revealed that (Al,Cr)$_3$Ti was more susceptible to amorphization. The consideration of chemical disordering only is not sufficient to explain the difference of susceptibility to amorphization between Al$_3$Ti and (Al,Cr)$_3$Ti under ion irradiation. Topological disordering needs to be considered together with chemical disordering to analyze the results obtained in this study. It is suggested that the addition of alloying elements promote the anti-site defect formation, which leads to an increase of the free energy. A previous study [21] showed that the critical dose to amorphization and the critical temperature varied according to the alloy type. This suggests that alloying elements play a critical role in defect accumulation under irradiation.

4. Conclusion

Samples of Al$_3$Ti and (Al,Cr)$_3$Ti were irradiated in situ with 1.0 MeV Kr ions at a rate of 6.25×10^{11} ions/cm^2-s at 40 K–573 K to doses up to 4.06×10^{15} ions/cm^2 to investigate the irradiation-induced disordering and amorphization of these compounds. The dose for completion of the irradiation-induced order-disorder transformation increased with increase in irradiation temperature, irrespective of the crystal structure, with both Al$_3$Ti and (Al,Cr)$_3$Ti ordered structures being fully transformed to the disordered FCC. Al$_3$Ti showed a higher irradiation dose to order-disorder transformation compared to (Al,Cr)$_3$Ti at a given temperature. However, the same disordered FCC structure showed a different tolerance to amorphization depending on the alloy. The disordered FCC-structured (Al,Cr)$_3$Ti amorphized at the irradiation dose of 6.25×10^{14} ions/cm^2 (0.92 dpa) at 40 K and 100 K. However, Al$_3$Ti with the disordered FCC structure maintained crystallinity up to an irradiation dose of 4.06×10^{15} ions/cm^2 (5.62 dpa) at 40 K.

References

[1] M. Yamaguchi, H. Inui, K. Ito, Acta Mater. 48 (2000) 307.
[2] M. Yamaguchi, Y. Shirai, in: Y.W. Kim, W.M. Griffith (Eds.), Dispersion Strengthened Aluminum Alloys, 1988, p. 721.
[3] Y. Nakayama, H. Mabuchi, Intermetallics 1 (1993) 41.
[4] A.E. Carlsson, P.J. Meschter, J. Mater, Res. 5 (1990) 2813.
[5] E.P. George, D.P. Pope, C.L. Fu, J.H. Schneibel, ISIJ Int. 31 (1991) 1063.
[6] S. Liu, R. Hu, D. Zhao, C. Wang, P. Luo, Z. Pu, J. Mater. Sci. Technol. 12 (1996) 180.
[7] M. Yamaguchi, H. Inui, in: J.H. Westbrook, R.L. Fleischer (Eds.), Intermetallic Compounds, 2, John Wiley, Chichester, UK, 1995, p. 147.
[8] A.E. Carlsson, P.J. Meschter, J. Mater. Res. 4 (1989) 1060.
[9] J.Y. Park, I.H. Kim, Y.I. Jung, H.G. Kim, D.J. Park, B.K. Choi, J. Nucl. Mater. 437 (2013) 75.
[10] D.B. Lee, S.H. Kim, K. Niinobe, C.W. Yang, M. Nakamura, Mater. Sci. Eng. A 290 (2000) 1.
[11] J.Y. Park, S.W. Park, H.N. Lee, M.H. Oh, D.M. Wee, Scr. Mater. 36 (1997) 801.
[12] C. Jaouen, M.F. Denenot, J.P. Riviere, Nucl. Instrum. Methods Phys. Res. B 80/81 (1993) 386.
[13] M. Nastasi, J.W. Mayer, Mater. Sci. Rep. 6 (1991) 1.
[14] A.T. Motta, J. Nucl. Mater. 244 (1997) 227.
[15] J.P. Biersack, L.G. Haggmark, Nucl. Instr. & Meth. 182/183 (1981) 199.
[16] G.H. Kinchin, R.S. Pease, J. Nucl. Energy 1 (1995) 200.
[17] D.E. Luzzi, M. Meshii, Res. Mech. 21 (1987) 207.
[18] A.T. Motta, D. Olander, Acta Met. Mater. 38 (1990) 2175.
[19] A.T. Motta, C. Lemaignan, in: A.R. Yavari (Ed.), Ordering and disordering in alloys, Elsevier Applied Science, London, NY, 1992, p. 255.
[20] K.E. Sickafus, R.W. Grimes, J.A. Valdez, A. Cleave, M. Tang, M. Ishimaru, S.M. Corish, C.R. Stanek, B.P. Uberuaga, Nat. Mater. 6 (2007) 217.
[21] A.T. Motta, J.A. Faldowski, L.M. Howe, P.R. Okamoto, Zirconium in the nuclear industry, in: E.R. Bradley, G.P. Sabol (Eds.), 11th International Symposium, ASTM STP 1295, 1996, p. 557. ASTM.